Results from the Averaging Model for Cuttings Transport in Horizontal Drilling

R. Salazar-Mendoza[1,] and A. García-Gutiérrez[2]

[1]Instituto Mexicano del Petróleo, Competencia de Producción de Hidrocarburos, Campeche, México
[2]Gerencia de Geotermia, Instituto de Investigaciones Eléctricas, Cuernavaca, Morelos, México
rsalazar@imp.mx

Keywords

Two-phase, cuttings transport, solid-liquid flow, drilling modeling, volume averaging

ABSTRACT

The Averaging Model for Cuttings transport in Horizontal Drilling was used to study the process of Cuttings transport for the three main flow patterns: Case I The fully suspended flow, Case II The flow with a stationary bed and Case III The flow with a moving bed. The models for all cases are in one-dimensional form. The one-dimensional models were solved numerically by using the finite difference technique in the implicit scheme. The numerical results were compared with experimental data and theoretical results reported in the literature and a good agreement was found.

Introduction

Due to the presence of two phases (solid and liquid) where the solid particles tend to settle at the bottom of the pipe (Doron and Barnea, 1993), the hydraulic transport of solid particles in horizontal pipes is a very complex physical phenomenon. Such phenomenon is relevant in several areas, such as the chemical, mining and oil industries.

In the oil industry, horizontal drilling is used to exploit reservoirs exhibiting thin pay zones, to solve the problems related to water and gas conning, to obtain greater drainage area, and to maximize the productive potential in naturally fractured reservoirs. However, a major deterrent in horizontal drilling is the reduction in performance of the transport of solid rocks fragments called cuttings transport (Cho *et al*., 2000).

Therefore, numerous mathematical and empirical models for the prediction of cuttings transport in horizontal and directional wells have been developed by several researchers (Salazar-Mendoza *et al.*, 2005; Salazar-Mendoza, 2004; Salazar-Mendoza *et al*., 2004; Cho *et al.*, 2002; Cho *et al.*, 2000; Li and Walker, 1999; Kamp and Rivero, 1999; Sanchez et al., 1999; Santana *et al*., 1998; Nguyen and Rahman, 1998; Leising and Walton, 1998; Doron *et al*., 1997; Azar and Sanchez, 1997; Pilehvari et al., 1996; Nguyen and Rahman, 1996; Martins *et al*., 1996).

A detailed review of published experimental data reveals that the cuttings transport characteristics change with an increase in wellbore angle. Leising and Walton (1998), Sifferman and Becker (1992) and Peden *et al*. (1990) reported that, under a certain range of well deviation, the cuttings bed in annuli is unstable. Tomren *et al.* (1986) and Ford *et al*. (1990) carried out experimental work on cuttings transport in inclined wellbores and observed the existence of different layers that might occur during the mud flow and cuttings in a wellbore: a stationary bed, a sliding bed, and a heterogeneous suspension or clear mud. Doron and Barnea (1996) carried out experimental work on solid-liquid flow in pipes and observed the existence of three main flow patterns: I Fully suspended flow, II Flow with a stationary bed and III Flow with a moving bed.

The aim of this paper is to present the results from the Averaging Model for Cuttings Transport in Horizontal Drilling, that was previously derived (Salazar-Mendoza *et al*., 2004; Salazar-Mendoza, 2004; Salazar-Mendoza *et al.*, 2005), and now it was used to study the process of Cuttings transport for the three main flow patterns: Case I The fully suspended flow, Case II The flow with a stationary bed and Case III The flow with a moving bed. The results have been used to predict the flow performance and to evaluate the effects of some important parameters which affect the mechanics of cuttings transport during horizontal well drilling. Also the numerical results were compared with experimental data from Doron *et al*. (1987) and experimental data and theoretical results from Doron and Barnea (1993).

Model Description

The system under consideration is illustrated in Figure 1, overleaf, where the fluid bed system is identified as the ω-region and the porous medium as the η-region. An exploded view of the ω-region that is made up of the solid phase (σ-phase)

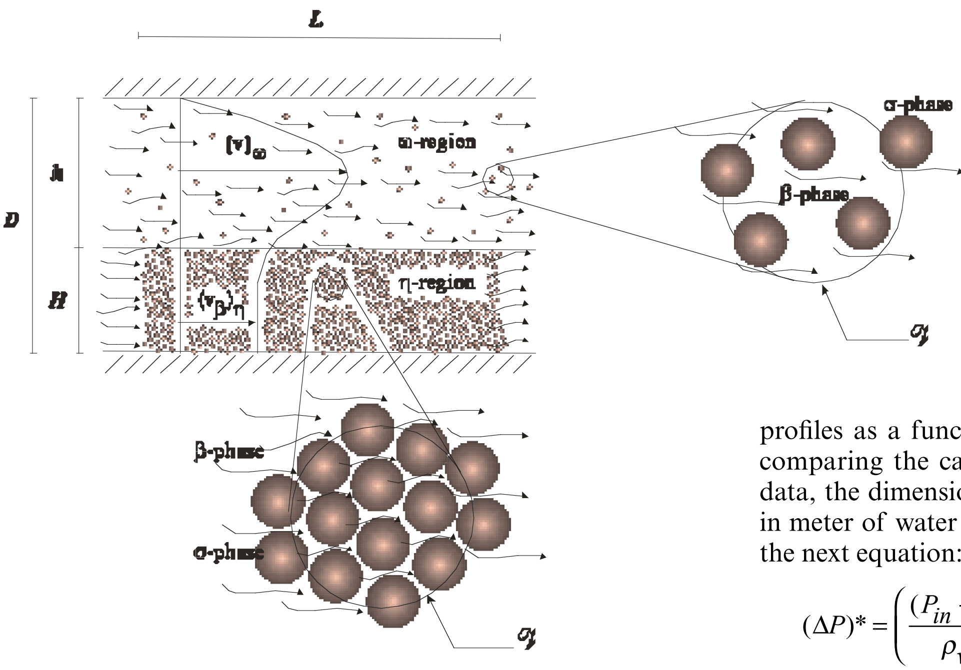

Figure 1. Cutting transport system and averaging volume.

dispersed in a continuous fluid phase (β-phase) is also shown in Figure 1. Additionally, an exploded view of the η-region that consists of a stationary solid phase (β-phase) and the fluid phase (β-phase) is shown there. Note that the β-phase is flowing in both ω and the η regions.

Results and Discussion

The simulated physical system is a pipe of 4.135 m in horizontal length and 0.0508 m in diameter. A one dimensional, mesh-centered grid, consisting of 10 nodes, is used for the three cases analyzed: Case I The fully suspended flow, Case II The flow with a stationary bed and Case III The flow with a moving bed.

In the first case, all the cross section of the pipe is occupied by a solid-liquid dispersed flow with a low concentration of drilling cuttings (like the ω-region in Figure 1). For the second case, a stationary bed of drilling cuttings (porous medium) is at the bottom of the pipe above which flows a flow similar to the Case I (Figure 1). For the third case, a moving bed of drilled cuttings with a high concentration of cuttings flow together a solid-liquid dispersed flow with a low concentration of cuttings. The models for all cases were obtained in one-dimensional form.

In order to solve the mathematical models, a backward finite difference implicit scheme with a point-distributed grid was applied. The set of equations for mass and momentum conservation in a discretized form can be written in matrix form as:

$$\mathbf{A} \cdot \mathbf{x} = \mathbf{b} \tag{1}$$

in which $\mathbf{A}$ is the matrix's coefficients, $\mathbf{x}$ is the vector of the dependent variables and $\mathbf{b}$ is the vector of the known parameters.

Case 1. Fully Suspended Flow

This type of flow pattern is presented at high superficial velocities (higher than 1.6 m/s). The liquid phase used in the simulation is water and the solid phase consists of particles with 0.003 m of diameter and a density of 1240 Kg/m^3 (data given in Doron et al., 1987). The pressure at the entrance of the pipe is 151988 Pa and the total volume fraction of solid particles ε_σ varies from 0.042 to 0.155

The aim of the numerical simulations is to obtain the pressure and velocity profiles as a function of time and space. With the idea of comparing the calculated pressure drop with experimental data, the dimensionless gradient pressure $(\Delta P)^*$ (expressed in meter of water by meters of pipe, m/m) is calculated with the next equation:

$$(\Delta P)^* = \left(\frac{(P_{in} - P_{out}) / L}{\rho_{water} g_r} \right) \tag{2}$$

where P_{in} and P_{out} are the pressure at the entrance of the pipe and the calculated pressure at the exit of the pipe, which length is L; P_{water} is the water density, and g_r is the gravity in the radial direction.

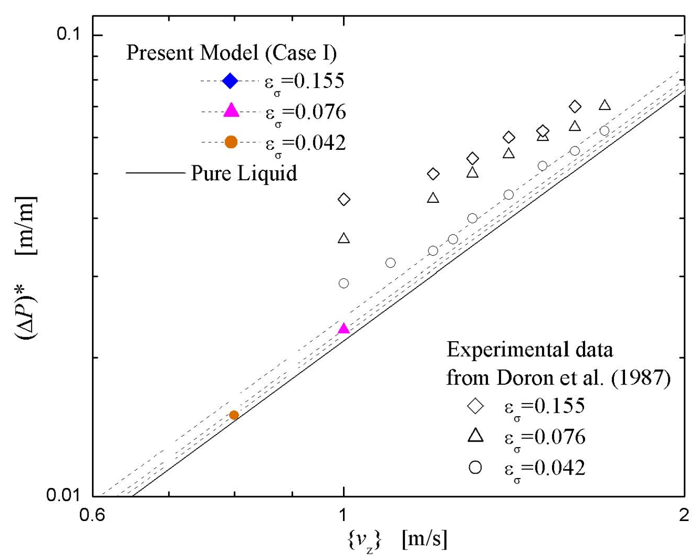

Figure 2. Dimensionless pressure gradient versus velocity for Case I A solid-liquid dispersed flow ($\rho_\sigma = 1240\,Kg/m^3$, $\rho_\beta = 1000\,Kg/m^3$, $d_p = 3$ mm , L = 4.135 m and D = 50 mm).

In Figure 2, the dimensionless pressure gradient versus velocity is presented. It can be observed that the prediction for various total volume fractions of drilling cuttings is similar that the results for a flow of pure liquid, which is due to the prediction was done with a homogeneous model, where the mixture properties are used. The predictions are compared with some experimental data from Doron et al., (1987), which were measured for superficial velocities approximately from 0.2 to 1.8 m/s. For these velocities the flow pattern observed was principally a flow with a moving bed, whereas only the data for superficial velocities higher than 1.6 m/s correspond to the fully suspended flow pattern. Therefore, the predictions are better when superficial velocities tend to high values. However, the predictions tend to move away respect to experimental data at low superficial velocities. Then, obviously the model is not adequate to simulate flow with a moving bed or a flow with a stationary bed, but it is appropriate for fully suspended flow prediction.

CASE 2. Flow with a Stationary Bed

Suppose a fully suspended flow in a horizontal pipe as the Case I. If the slurry flow rate is reduced, the solid particles tend to form a moving bed at the bottom of the pipe (due to density is higher than that of the carrier fluid). Decreasing the flow rate further, the solid particles tend to form a stationary bed instead of a moving bed.

The flow with a stationary bed was simulated using the same data that for Case I and a value for the total volumetric fraction of solid particles ε_σ of 0.097.

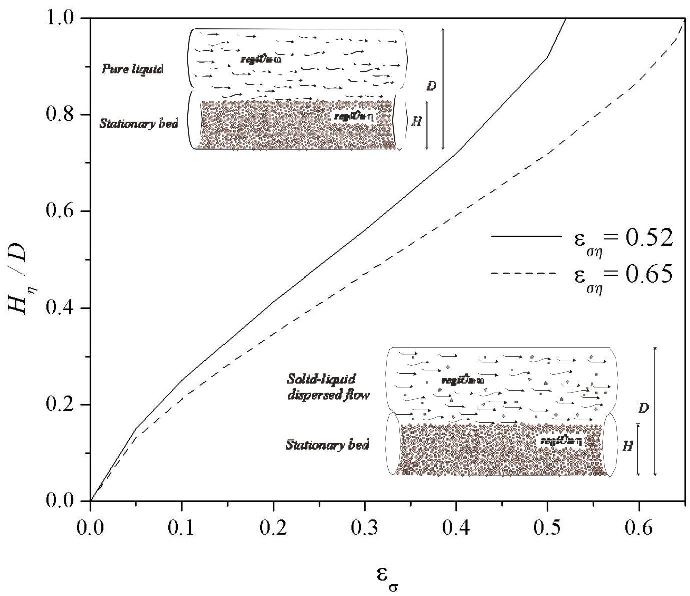

Figure 3. Flow pattern transition for a two-region model as a function of the total volume fraction of drilling cuttings and the maximum packing at the bottom of the pipe.

With the model and values of 0.52 and 0.65 for the maximum packing at the bottom of the pipe $\varepsilon_{\sigma\eta}$, the Figure 3 was obtained. This figure shows the relation *H / D* as a function of ε_σ and $\varepsilon_{\sigma\eta}$, obtaining the flow pattern transition for a solid-liquid two phase flow. From Figure 3, it can be observed that: 1) the point (0,0) represents one phase flow, 2) the points (ε_σ, 0) represent fully suspended flow, 3) the points (0.52, 1) and (0.65,1) represent flow through a porous medium (stationary bed) and 4) with the other points; it is possible to predict if the upper region is a fully suspended flow or only a flow of pure liquid when the bottom region is a stationary bed or a moving bed.

For this case the dimensionless gradient was calculated by

$$(\Delta P)^* = \varepsilon_\omega (\Delta P)^*_\omega + \varepsilon_\eta (\Delta P)^*_\eta \tag{3}$$

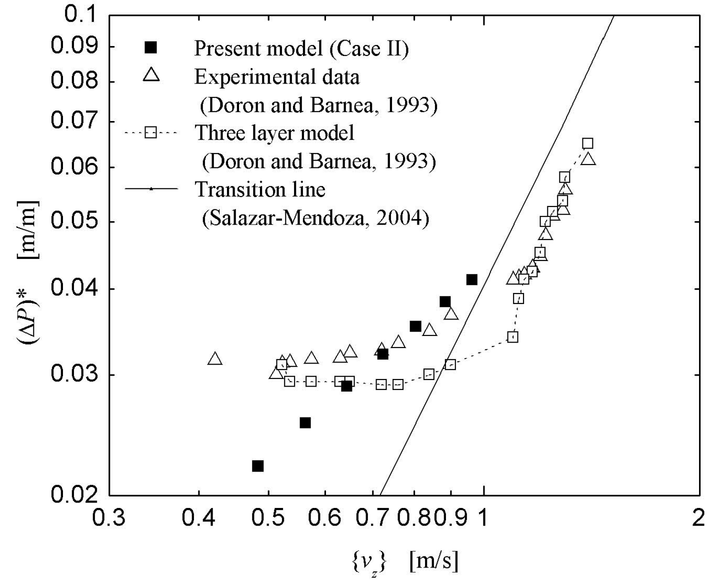

Figure 4. Dimensionless pressure gradient versus velocity for Case II A flow with a stationary bed. Comparison of two-region model against experimental data and three –layer model from Doron and Barnea (1993) ($\rho_\sigma = 1240\,\mathrm{Kg/m^3}$, $\rho_\beta = 1000\,\mathrm{Kg/m^3}$, $d_p = 3$ mm , L = 4.135 m y D = 50 mm, $\varepsilon_\sigma = 0.097$).

where $(\Delta P)^*_\omega$, $(\Delta P)^*_\eta$, ε_ω and ε_η are the dimensionless pressure gradients and the volume fractions for the ω and η regions, respectively.

In Figure 4 the theoretical transition between flow with a stationary bed (left side of the continuous line) and flow with a moving bed (right side of the continuous line) are shown. In this figure, can be observed that numerical results for $(\Delta P)^*$ are in agreement with the profile of experimental data and the Doron and Barnea model in the velocity range from 0.6 to 0.95 m/s. The maximum error calculated between the numerical and experimental data was 5%.

With the idea of evaluating the behavior of the volume fraction of cuttings in the upper region $\varepsilon_\sigma\omega$ as a function of: ε_σ, $\varepsilon_{\sigma\eta}$, and *H / D*, the next equation was used

$$\varepsilon_{\sigma\omega} = (\varepsilon_\sigma - \varepsilon_{\sigma\eta}\varepsilon_\eta) / \varepsilon_\omega \tag{4}$$

In Figure 5, overleaf, all the points on the $\varepsilon_\sigma\omega$-axis (i.e., *H / D=0*) represent fully suspended flow and all the points on the *H / D*-axis (i.e., $\varepsilon_\sigma\omega = 0$) represent flow through a porous medium (stationary bed) with a flow of only liquid phase at the top of the pipe. The other points on solid and dashed lines represent flow with a stationary bed (like in Figure 1).

In Figure 6, overleaf, the dimensionless pressure gradient as a function of volume averaged velocity and the relation *H / D* is presented. It can be observed that, for a constant velocity, if the relation *H / D* grows up then, also, the dimensionless pressure gradient grows up. In the practice and experimentally it is very difficult to maintain the relation *H / D* constant, however with Figure 6 it is possible to predict how the behavior of the dimensionless pressure gradient is as a function of volume averaged velocity.

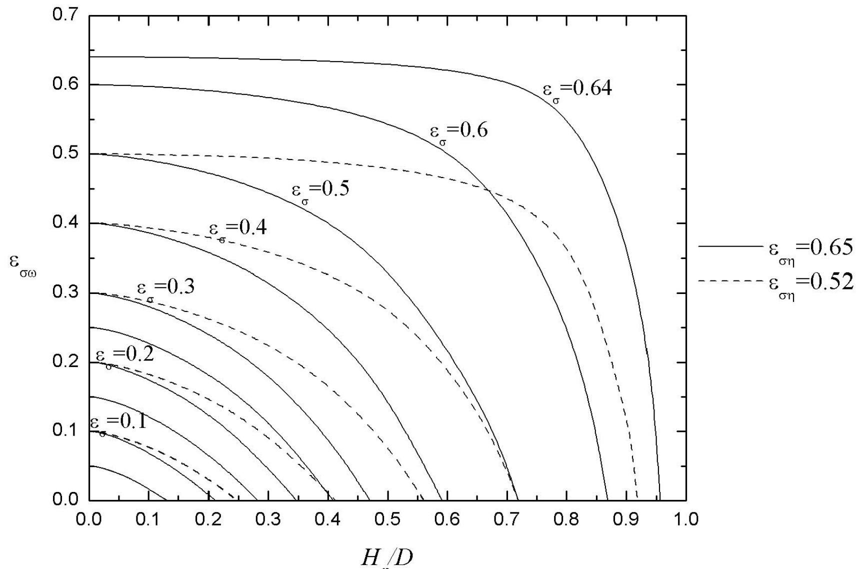

Figure 5. Behavior of volume fraction of drilling cuttings at the top of the pipe as a function of: 1) the total volume fraction of drilling cuttings, 2) the maximum packing at the bottom of the pipe, and 3) the relation H/D.

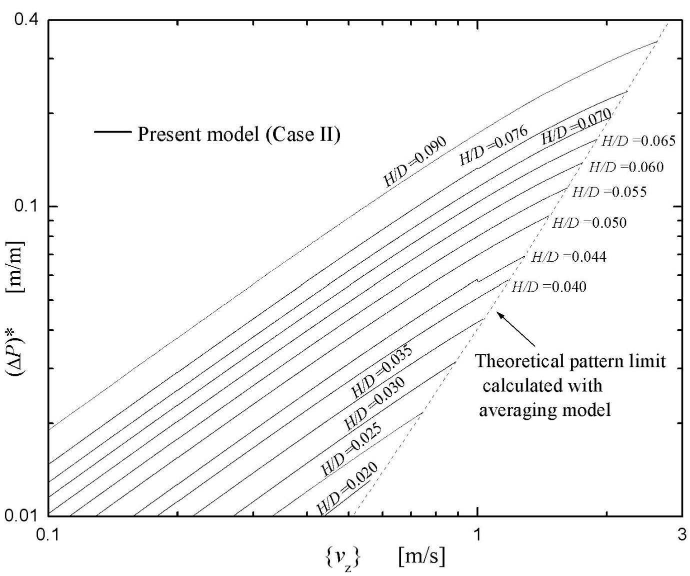

Figure 6. Dimensionless pressure gradient versus velocity $\{v_z\}$ for Case II A flow with a stationary bed for different values of the relation H/D.

CASE 3. Flow with a Moving Bed

Suppose a fully suspended flow in a horizontal pipe as the Case I. If the slurry flow rate is reduced, the solid particles tend to form a moving bed at the bottom of the pipe (due to density is higher than that of the carrier fluid). Decreasing the flow rate further, the solid particles tend to form a stationary bed instead of a moving bed.

The flow with a moving bed is a intermediate flow pattern between the fully suspended flow and the flow with a stationary bed. This kind of flow was simulated using the same data that for Case I and a value for the total volumetric fraction of solid particles ε_σ of 0.11.

In this case the dimensionless gradient was calculated by

$$(\Delta P)^* = \varepsilon_\omega (\Delta P)^*_\omega + \varepsilon_\gamma (\Delta P)^*_\gamma \tag{5}$$

where $(\Delta P)^*_\omega$, $(\Delta P)^*_\gamma$, ε_ω and ε_γ are the dimensionless pressure gradients and the volume fractions for the ω and γ regions, respectively.

In Figure 7 the transition between flow with a moving bed (right side of the continuous line) and flow with a stationary bed (left side of the continuous line) are shown. In this figure, can be observed that numerical results for $(\Delta P)^*$ are in agreement with the profile of experimental data taken from Doron and Barnea (1993) in the velocity range from 1.0 to 1.6 m/s. The maximum error calculated between the numerical and experimental data was 6.8%.

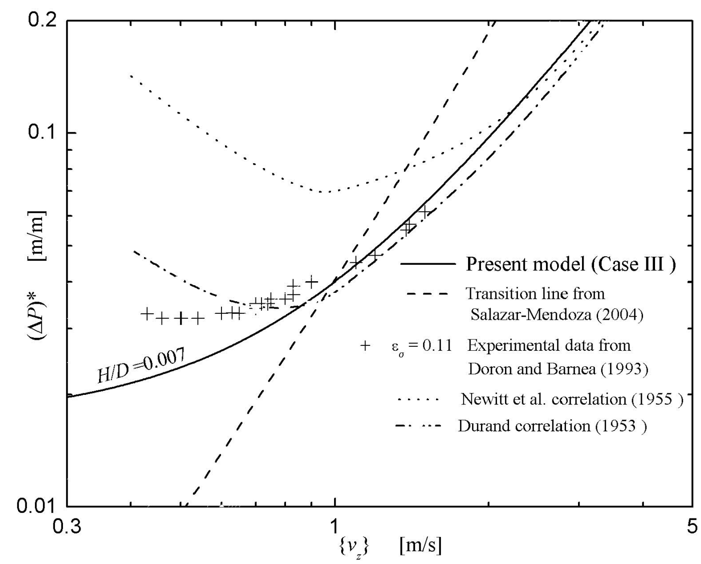

Figure 7. Dimensionless pressure gradient versus velocity for Case III A flow with a moving bed. Comparison of two-region model against correlations and experimental data and three –layer model from Doron and Barnea (1993) ($\rho_\sigma = 1240\,\mathrm{Kg/m^3}$, $\rho_\beta = 1000\,\mathrm{Kg/m^3}$, $d_p = 3$ mm , L = 4.135 m y D = 50 mm, $\varepsilon_\sigma = 0.11$).

Conclusions

In this work, the process of cutting transport for the three main flow patterns was analyzed: 1) fully suspended flow, 2) flow with a stationary bed, and 3) flow with a moving bed. The numerical results and their comparison with experimental data and theoretical results show that: 1) the model for a fully suspended flow is not adequate for simulating a flow with a moving bed nor a flow with a stationary bed, 2) the models for a flow with a stationary bed and a flow with moving bed allow to obtain the theoretical flow pattern transition, as a function of total volume fraction, which depends on the maximum packing at the bottom of the pipe, 3) the results for the dimensionless pressure gradient, obtained for a flow with a stationary bed and a flow with a moving bed, are in agreement with experimental data and theoretical results reported in the literature, as is illustrated in Figures 4 and 7.

Acknowledgements

This research was made possible by support from the Instituto Mexicano del Petróleo (IMP) and Consejo Nacional de Ciencia y Tecnologia (CONACyT) of México.

Nomenclature

d_p	particle diameter
D	pipe diameter
$H\eta$	height of the η-region, for the case of stationary bed
$H\gamma$	height of the γ-region, for the case of moving bed
h	height of the ω-region
L	pipe length
$(\Delta P)^*$	dimensionless pressure gradient
P_{in}	pressure at the entrance of the pipe
P_{out}	pressure at the exit of the pipe
$\mathcal{V}$	averaging volume
V_β	volume of the β-phase contained in the averaging volume
V_σ	volume of the σ-phase contained in the averaging volume

Greek Symbols

β	fluid phase
δ	boundary layer thickness
ε_β	$=\dfrac{V_\beta}{\mathcal{V}}$, volume fraction of the β-phase
ε_σ	$=\dfrac{V_\sigma}{\mathcal{V}}$, volume fraction of the σ-phase
$\varepsilon_{\sigma\omega}$	volume fraction of the σ-phase associated with the ω region
$\varepsilon_{\sigma\eta}$	volume fraction of the σ-phase associated with the η region (stationary bed)
$\varepsilon_{\sigma\gamma}$	volume fraction of the σ-phase associated with the γ region (moving bed)
γ	moving bed
η	stationary bed, porous medium
ρ_β	density in the β-phase
ρ_σ	density in the σ-phase
σ	solid phase
ω	fluid bed system

Subscripts

γ	identifies a quantity associated with the γ region
η	identifies a quantity associated with the η region
$\omega\gamma$	identifies a quantity associated with the ω-γ boundary
$\omega\eta$	identifies a quantity associated with the ω-η boundary
β_γ	identifies the fluid phase in the γ-region
β_η	identifies the fluid phase in the η-region
β_ω	identifies the fluid phase in the ω-region
$\sigma\gamma$	identifies the solid phase in the γ-region
$\sigma\eta$	identifies the solid phase in the η-region
$\sigma\omega$	identifies the solid phase in the ω-region
ω	identifies a quantity associated with the ω region

References

Azar, J. J., and R. A. Sanchez, 1997. Important Issues in Cuttings Transport for Drilling Directional Wells. Fifth Latin American and Caribbean Petroleum Engineering Conference and Exhibition, Rio de Janeiro, Brazil, Aug. 30–Sept. 3. SPE Paper 39020.

Cho H., S. N. Shah, and S. O. Osisanya, 2002. A Three-Segment Hydraulic Model for Cuttings Transport in Coiled Tubing Horizontal and Deviated Drilling. J. of Canadian Petroleum Technology, v. 41(6), p. 32-39.

Cho, H., S. N. Shah, and S. O. Osisanya, 2000. A Three-Layer Modeling for Cuttings transport with Coiled Tubing Horizontal Drilling. SPE Annual Technical Conference and Exhibition, Dallas, TX, October 1-4. SPE Paper 63269.

Doron, P., D. Granica, and D. Barnea, 1987. Slurry Flow in Horizontal Pipes-Experimental and Modeling. Int. J. Multiphase Flow, v. 13(4), p. 535-547.

Doron, P., and D. Barnea, 1993. A Three-Layer Model for Solid-Liquid Flow in Horizontal Pipes. Int. J. Multiphase Flow, v. 19(6), p. 1029-1043.

Doron, P., and D. Barnea, 1996. Flow pattern maps for solid-liquid flow in pipes. Int. J. Multiphase Flow, v. 22 (2), p. 273-283.

Doron, P., M. Simkhis, and D. Barnea, 1997. Flow of Solid-Liquid Mixtures in Inclined Pipes. Int. J. Multiphase Flow, v. 23(2), p. 313-323.

Ford, J.T., J.M. Peden, E.G. Oyeneyin, and R. Zarrough, 1990. Experimental Investigation of Drilled Cuttings Transport in Inclined Boreholes. SPE Annual Technical Conference, New Orleans, Sept. 23-26. SPE Paper 20421.

Kamp, A. M., and M. Rivero, 1999. Layer Modeling for Cuttings Transport in Highly Inclined Wellbores. SPE Latin American and Caribbean Petroleum Engineering Conference, Caracas, Venezuela, April 21-23. SPE Paper 53942.

Leising, L.J., and I.C. Walton, 1998. Cuttings Transport Problems and Solutions in Coiled Tubing Drilling. IADC/SPE Drilling Conference, Dallas, TX, March 3-6. SPE Paper 39300.

Li, J., and S. Walker, 1999. Sensitive Analysis of Hole Cleaning Parameters in Directional Wells. SPE/ICoTA Coiled Tubing Roundtable, Houston, TX, May 25-26. SPE Paper 54498.

Martins, A.L., C.H.M. Sá, A.M.F. Lourenço, L.G.M. Freire, and W. Campos, 1996. Experimental Determination of Interfacial Friction Factor in Horizontal Drilling With a Bed of Cuttings. SPE Latin American and Caribbean Petroleum Engineering Conference, Port of Spain, Trinidad & Tobago, April 23-26. SPE Paper 36075.

Nguyen, D., and S.S. Rahman, 1996. A Three-Layer Hydraulic Program for Effective Cuttings Transport and Hole Cleaning in Highly Deviated and Horizontal Wells. IADC/SPE Asia Pacific Drilling Technology, Kuala Lumpur, Malaysia, Sept. 9-11. SPE Paper 36383.

Nguyen, D., and S.S. Rahman, 1998. A Three-Layer Hydraulic Program for Effective Cuttings Transport and Hole Cleaning in Highly Deviated and Horizontal Wells. SPE Drilling & Completion, 182-189 (Sept.). SPE Paper 51186.

Peden, J.M., J.T. Ford, and M.B. Oyeneyin, 1990. Comprehensive Experimental Investigation of Drilled Cuttings Transport in Inclined Wells Including the Effects of Rotation and Eccentricity. Europe 90, The Hague, Netherlands, October 22-24. SPE Paper 20925.

Pilehvari, A.A., J.J. Azar, and S.A. Shirazi, 1996. State-of-the-Art Cuttings Transport in Horizontal Wellbores. International Conference on Horizontal Well Technology, Calgary, Canada, Nov. 18-20. SPE Paper 37079.

Salazar-Mendoza, R., G. Espinosa-Paredes, A. García, O. Cazarez-Candia, A. Díaz, and A. Vázquez, 2004. "Averaging Model for Cuttings Transport in Horizontal Drilling", Geothermal Resources Council Transactions, v. 28, p. 169-175.

Salazar-Mendoza, R., 2004. Modelo Hidrodinámico para el Estudio del Transporte de Recortes de Perforación en la Sección Horizontal de Pozos Petroleros. Tesis de Doctorado. Departamento de Mecánica, CENIDET, Cuernavaca, Morelos, México.

Salazar-Mendoza, R., G. Espinosa-Paredes, O. Cazarez-Candia, E. G. Espinosa-Martinez, A. Aragón-Jerónimo, and A. Vázquez 2005. "A Two-Region Averaging Model for Solid-Liquid Flow in Horizontal Pipes". Proceedings of 4th International Conference on Computational Heat and Mass Transfer, May 17-20, Paris-Cachan, France, v. 1, p. 319-322.

Sanchez, R.A., J.J. Azar, A.A. Bassal, and A.L. Martins, 1999. Effect of Drillpipe Rotation on Hole Cleaning During Directional Well Drilling. SPE Journal, v. 4(2), p. 101-107. SPE Paper 56406.

Santana, M., A.L. Martins, and A. Sales, 1998. Advances in the Modeling of the Stratified Flow of Drilled Cuttings in High Angle and Horizontal Wells. SPE International Petroleum Conference and Exhibition, Villahermosa Tabasco, Mexico, March 3-5. SPE Paper 39890.

Sifferman, T.R. T.E. and Becker, 1992. Hole Cleaning in Full-Scale Inclined Wellbores. SPE Drilling Engineering, (June). p. 115-120. SPE Paper 20422.

Tomren, P.H., A.W. Iyoho, and J.J. Azar, 1986. An Experimental Study of Cuttings Transport in Directional Wells. SPE Drilling Engineering, (Feb.). p. 43-56. SPE Paper 12123.